5-2003

Finite Element Studies in Metal Cutting

Suhail Ahmed
Utah State University

FINITE ELEMENT STUDIES IN METAL CUTTING

by

Suhail Ahmed

A report submitted in partial fulfillment
of the requirements for the degree

of

MASTER OF SCIENCE

in

Industrial Mathematics

UTAH STATE UNIVERSITY
Logan, Utah

2003

ABSTRACT

Finite Element Studies in Metal Cutting

by

Suhail Ahmed, Master of Science

Utah State University, 2003

Major Professor: Dr. Emily Stone
Department: Mathematics and Statistics

AdvantEdge is a finite element software package that integrates advanced dynamics, thermo-mechanically coupled finite element numerics and material modelling appropriate for machining processes. AdvantEdge allows users to specify the workpiece material, tool geometry and cutting conditions. It then provides accurate estimates of thermo-mechanical properties of machining processes such as cutting forces, chip morphology, machined surface residual stresses and temperature behavior of the tool and the workpiece. We will use AdvantEdge to investigate two areas of interest in metal cutting: process damping via crushing of workpiece material and drilling of metal stacks.

(40 pages)

DEDICATION

I would like to dedicate this report to my parents Zakira and Abdul Saleem and my little sister Sumaiya. Thank you for your patience, love and support.

ACKNOWLEDGMENTS

This thesis would not have been possible without the help of a number of people. Dr. Emily Stone for her patience and help, Hong Tat with the MEA group in Boeing, my committee members Dr. Kathryn Turner and Dr. Ning Fang and finally Bruce Mowrer from the Boeing Library, Renton for his timely assistance with literature searches.

Suhail Ahmed

CONTENTS

LIST OF TABLES

LIST OF FIGURES

Metal cutting is one of the most common operations in manufacturing. It involves the removal of undesired material in the form of chips from the workpiece to obtain the finished product. The purpose of the project reported here was to investigate the behavior of forces acting on the tool and the work materials during metal cutting. The report is divided into two parts. The first part describes process damping forces acting on the tool, their behavior, relationship with other cutting parameters and how these could be modelled. The second part is a study of the modelling of drilling metal stacks. In both sections of the report we make use of a finite element machining software to analyze the given problem and obtain relevant results.

CHAPTER 1
MODELLING PROCESS DAMPING: CRUSHING FORCES

1.1 INTRODUCTION TO PROCESS DAMPING: CRUSHING FORCES

One of the biggest problems faced in metal cutting is the presence of chatter or vibrations. Ideally the work material is homogeneous and has the same material properties throughout. In reality, material properties do not remain constant, and hard spots exist. When the tool hits such a hard spot, it is disturbed which can result vibrations of the tool. These vibrations may die down, or vibrations (chatter) may continue. Chatter leads to undesirable consequences such as poor surface quality and early wear of the tool, which causes loss in structural performance of the aircraft or expensive rework.

There are a number of forces acting on the tool as it cuts metal. The primary force can be resolved into a cutting force and the thrust force. Additionally there are effects that contribute to dissipation of energy, for example, rubbing of work material on the tool. These effects are collectively called process damping. In figure 1.1, a two dimensional view of the the tool cutting metal as it moves from the right to the left, illustrates the tool geometry. The face over which the cut material, in the form of chips, moves is called as the rake face of the tool and is inclined to the vertical at an angle α, called the tool rake angle. The bottom of the tool just above the cut workpiece surface is called the relief face. It is inclined to the horizontal to minimize contact with the workpiece. However contact is likely to occur if the tool is experiencing chatter. Such contact leaves behind a flattened or crushed work surface. The force associated with such crushing of the workpiece by the tool relief face is what we call the crushing force and contributes to process damping.

The crushing force plays an important role in process dynamics, especially on the stability of vibrations. Brian Whitehead incorporated process damping into a model of chatter during drilling [7]. His model was our starting point in studying crushing forces. Here Whitehead assumed an inverse relationship between the magnitude of crushing forces and

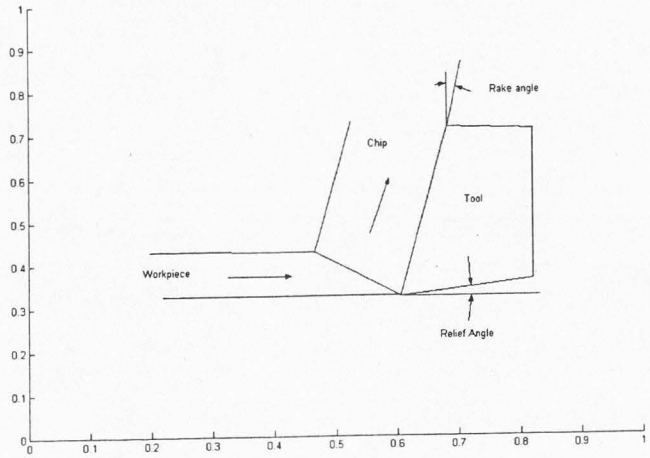

Figure 1.1. Tool Geometry

wavelength of vibration because smaller wavelengths lead to greater crushing contact with workpiece causing higher crushing forces. In this report we simulate crushing behavior using validated finite element software called AdvantEdge to test the assumption made by Whitehead and investigate modelling of crushing forces based on contact length between tool relief face and workpiece.

1.2 CRUSHING SIMULATION AND RESULTS

1.2.1 Introduction to AdvantEdge

Investigation of the crushing forces was done with machining simulation software called AdvantEdge, developed by Third Wave Systems, Inc. [6]. AdvantEdge is a finite element software package that integrates advanced dynamics, thermo-mechanically coupled finite element numerics and material modelling appropriate for machining processes. AdvantEdge allows users to specify the workpiece material, tool geometry and cutting conditions. It then provides accurate estimates of thermo-mechanical properties of machining processes such as cutting forces, chip morphology, machined surface residual stresses and temperature behavior of the tool and the workpiece [5].

In our investigation, we made use of a new module within AdvantEdge that allows the tool to be vibrated. As explained in section 1, crushing is likely during chatter and the vibrating tool feature is used to simulate crushing behavior.

1.2.2 Method

In order to compute crushing forces, two almost identical simulations (same workpiece and the same cutting conditions) were run for tools of three relief lengths, with a difference in the tool relief angles. In the first, the relief angle was small enough so that the relief face of the tool crushed the work material as it moved through the cut. In the second simulation, the relief angle was made large enough so that there was very little contact between the relief face of the cutter and the work material. Assuming that the forces involved in material removal and crushing combine linearly, the crushing force was resolved by subtracting the forces from two such runs [5].

Figures 1.2 and 1.3 show the parameters of the simulations. Figure 1.4 is a snapshot of a crushing simulation where the tool has crushed the workpiece on its sinusoidal path. One can clearly see the flattened regions. The resultant force acting on the tool have a crushing component. In this study we are only considering the vertical crushing component.

Figure 1.5 illustrates the same work material being cut under the same cutting conditions except that the tool relief angle has been changed from 6 degrees to 25 degrees, so that there is little contact between the tool relief face and the work material, and the tool tip leaves a sinusoidal workpiece surface in its wake. In this simulation forces acting on the tool have a very small crushing component. Subtracting the forces in the vertical direction from the two simulations will give us the crushing component.

A plot of the crushing forces is illustrated in figure 1.6, where the material being cut is

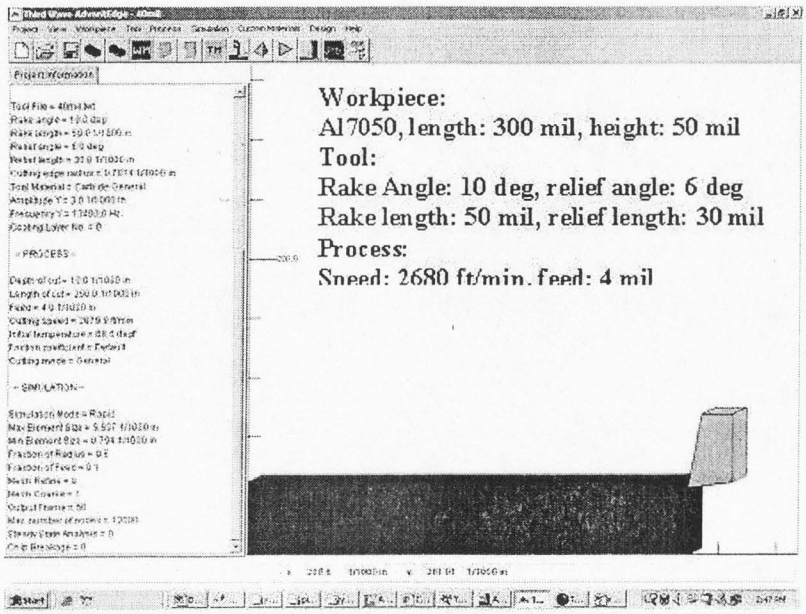

Figure 1.2. Simulation set up for crushing run.

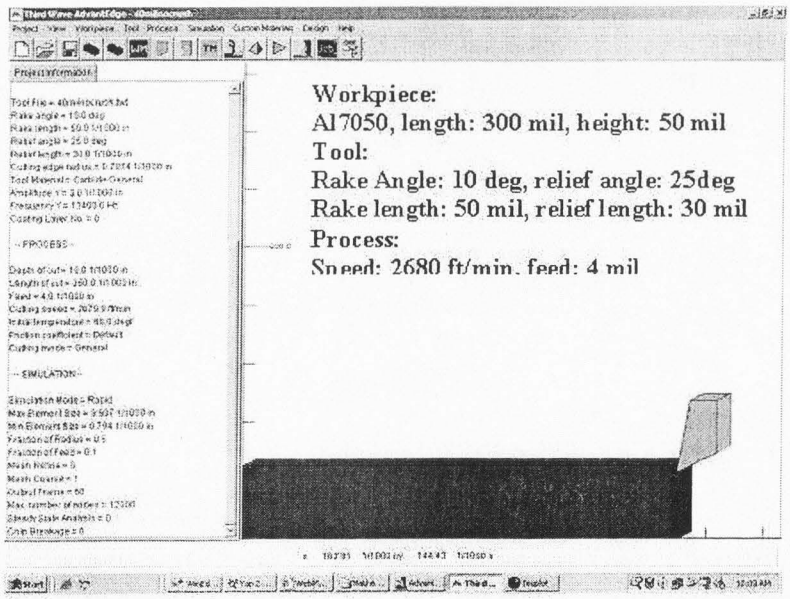

Figure 1.3. Simulation set up for non-crushing run.

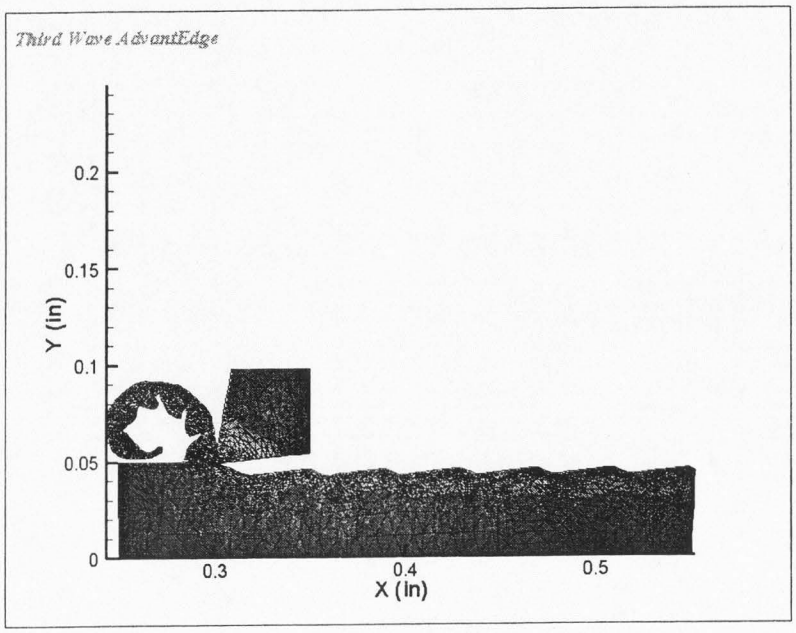

Figure 1.4. Crushing Run - Simulation.

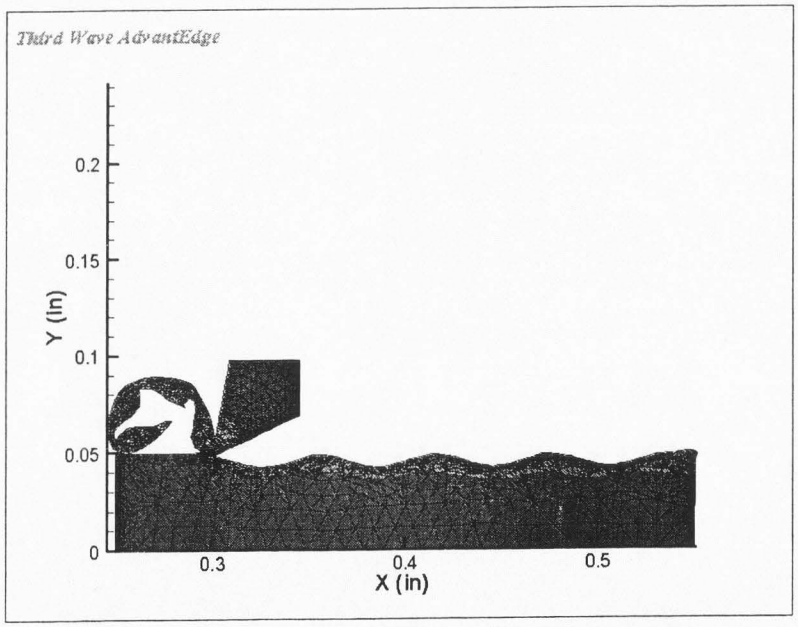

Figure 1.5. Non-crushing run simulation.

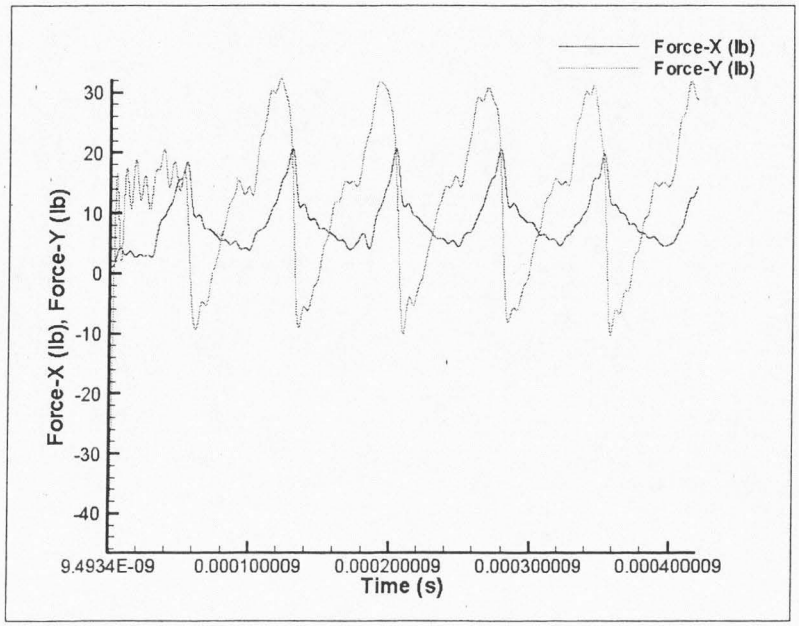

Figure 1.6. Forces occurring in crushing simulation.

Al 7050, with a carbide tool with a 10 degree rake angle and a cutting edge radius of 0.7874 mils. In the two simulations, the tool vibrates with a wavelength of 40 mils, corresponding to a cutting speed of 2680 SFM (surface feet/min) and a vibration frequency of 13.4 KHz with an amplitude of 3 mil (typical of axial-torsional vibration mode of a drill). The x-axis represents the time for which the tool has been cutting the material. The y-axis represents the forces acting in the horizontal (F-x) and vertical (F-y) directions. The force in the horizontal direction acting on the tool is referred to as the cutting force. The force on the tool in the vertical direction is referred to as the thrust force. The crushing component in the vertical direction alone is considered in this study.

1.2.3 Modelling Crushing Forces with Contact Length

We postulate that the magnitude of crushing forces will depend on the area of material being crushed under the tool or the contact length. Figure 1.7 represents a short relief length tool moving on a sinusoidal path as it moves from the left to the right. Figure 1.8 illustrates

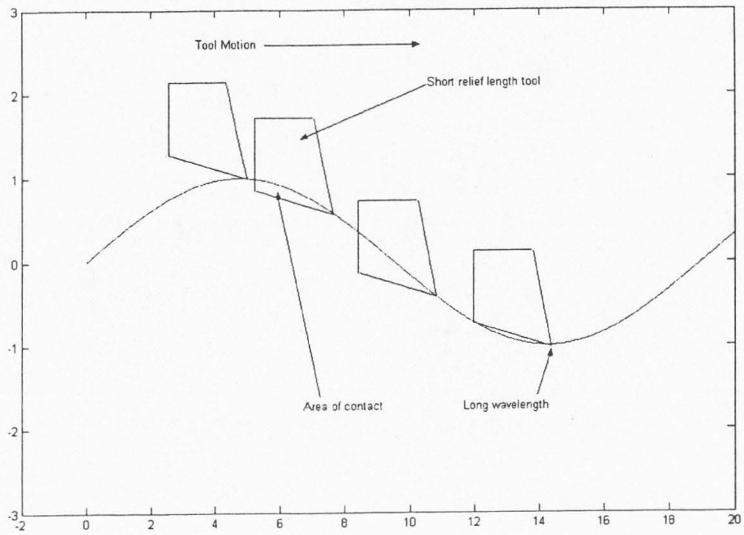

Figure 1.7. Variation of contact length during cutting for short relief length tool-long wavelength

that as wavelength of oscillation decreases, contact length saturates but the area of work material being crushed under the tool increases causing larger crushing forces, implying an inverse dependence of forces on wavelength, as Whitehead assumed. This suggests that a contact area model may work for the short relief tool. Figures 1.9 and 1.10 illustrates the crushing motion of a long relief length tool. Here a increase in the wavelength of oscillation causes longer contact length between tool relief face and workpiece suggesting a contact length model. Simulations were therefore run with varying tool relief lengths with varying wavelengths in order to understand the effect of contact length and wavelength on the behavior of crushing forces. The results are presented in section 1.3.

1.3 Results

In this section we present results of simulations to investigate crushing forces. Simulations were run for the following tool relief lengths.

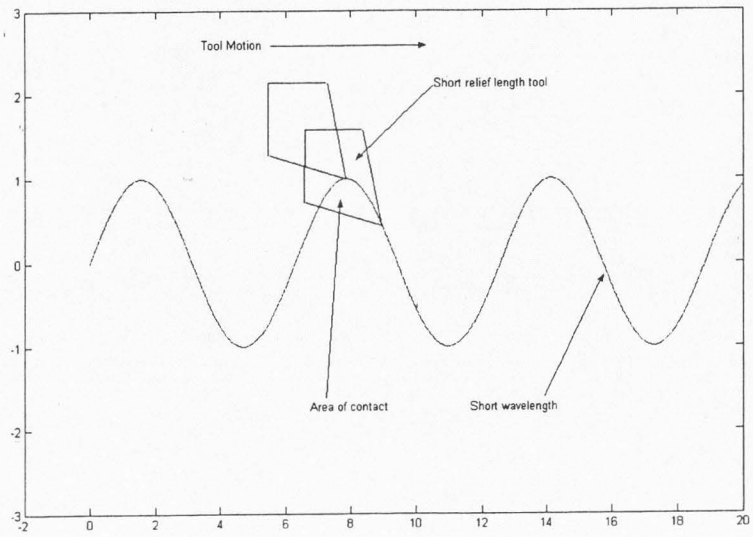

Figure 1.8. Variation of contact length during cutting for short relief length tool-short wavelength

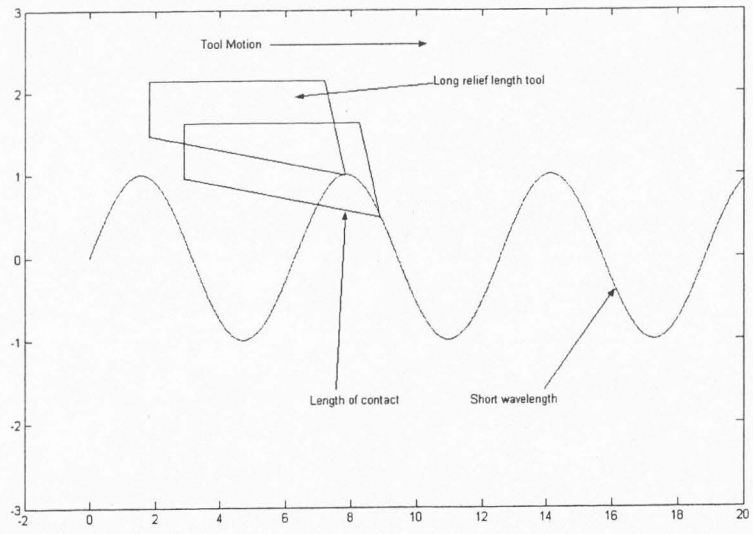

Figure 1.9. Variation of contact length during cutting for long relief length tool-short wavelength

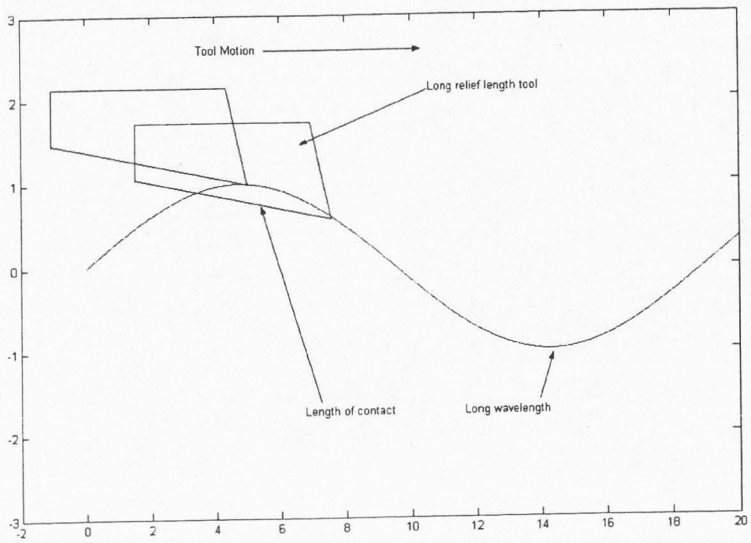

Figure 1.10. Variation of contact length during cutting for long relief length tool-long wavelength

1. Short relief length tool - 10 mil
2. Intermediate relief length tool - 30 mil
3. Long relief length tool - 80 mil

The tool in each simulation was vibrated at varying wavelengths (40mil, 60 mil, 80 mil and 100 mil). As explained in section 1.2.2, in order to compute crushing forces we simulate the tool through a crushing and a non-crushing run for each of the specified wavelengths. Each of these simulations had the following cutting conditions

1. Workpiece
   (a) Length: 300 mil
   (b) Height: 50 mil
   (c) Material: Al 7050
2. Tool

(a) Material: Carbide

(b) Rake angle: 10 mil

(c) Cutting Edge Radius: 0.7874 mil

3. Process

(a) Length of Cut: 250 mil

(b) Depth of Cut: 4 mil

(c) Cutting Speed: 2680 SFM

(d) Vibration frequency: variable

(e) Vibration Amplitude: 3 mil

1.3.1 Behavior of crushing forces

As In this section we will test Whitehead's assertion that crushing forces are inversely proportional to the wavelength of vibration. Figure 1.11 represents a plot of crushing forces on the relief face of the tool *vs.* the vertical position of a short relief tool length (10 mil). Simulations were performed for different wavelengths of vibration of the tool: 40 mil, 60 mil, 80 mil and 100 mil. For each simulation we allowed the tool to vibrate through at least two complete cycles. This is the reason for each wavelength having more than one loop in figure 1.11. The x-axis represents the vertical position of the tool through a sinusoidal undulation with amplitude 3 mils. The crushing forces go to zero at the bottom of the loop as the tool moves from its lowest position to its peak. Past the peak position the relief face starts coming into contact with the work material, at an amplitude that depends on the wavelength causing an increase in crushing forces. The loops in the plots are traversed counter-clockwise and the maximum force increases with *decreasing* wavelength. Note that the bold lines represent the 100 mil wavelength simulation and are actually a set of asterisks closely spaced so that they look like bold lines.

In figure 1.12, representing simulations with a long relief tool length(80 mil), we see that the crushing force in the y direction increases during the downward motion of the tool,

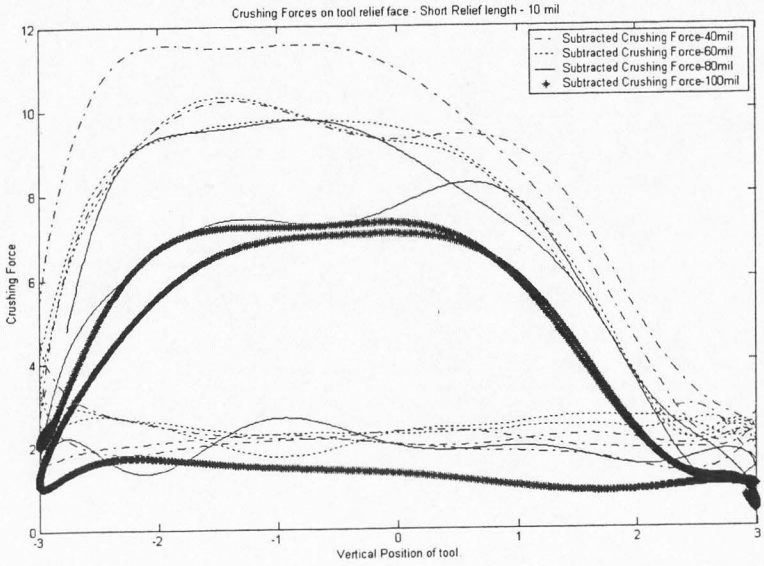

Figure 1.11. Crushing forces vs. vertical position of short relief length tool (10 mil).

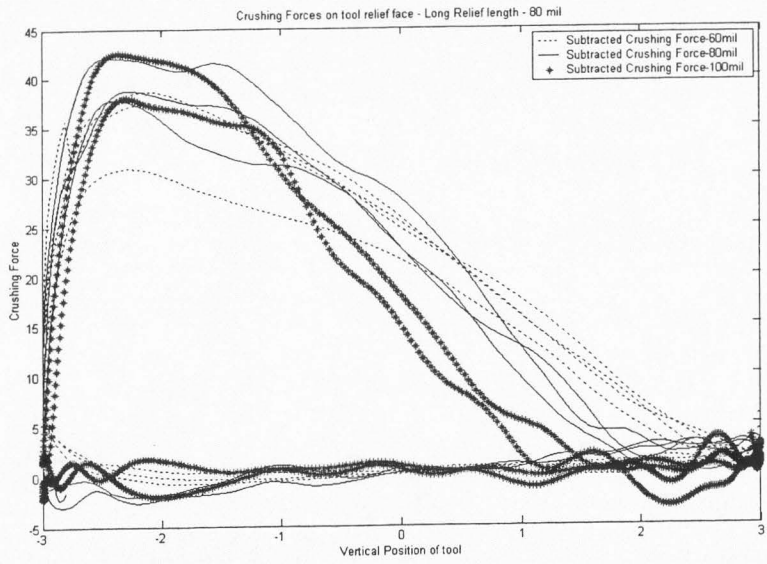

Figure 1.12. Crushing forces vs. vertical position of long relief length tool (80 mil).

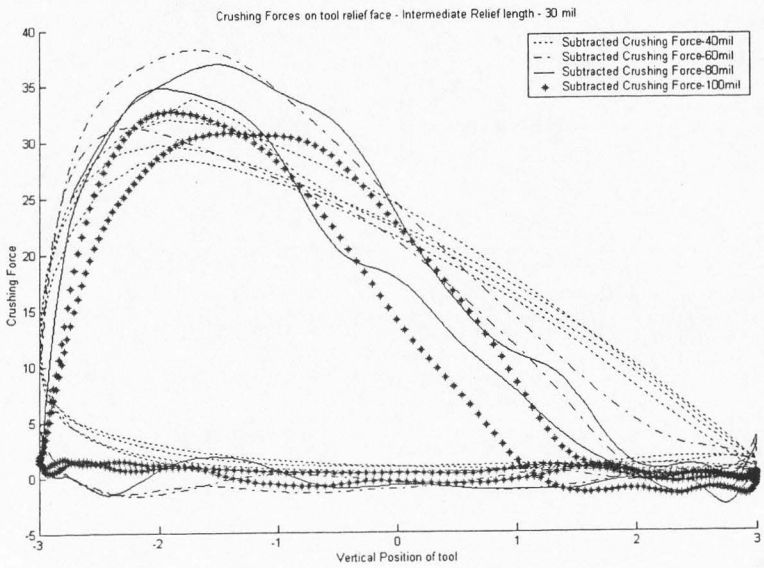

Figure 1.13. Crushing forces vs. vertical position of intermediate relief length tool (30 mil).

but now the maximum force increases with *increasing* wavelength. Note however, that the maximum crushing forces for the 80 mil and 100 wavelength are almost the same.

Figure 1.13 shows a similar plot of crushing forces *vs.* the vertical position of the tool for a tool having a relief face length of 30 mil. The relationship between the crushing forces and the wavelength is less clear than for the short and long relief length tool.

1.3.2 Crushing Forces vs Contact Length

The magnitude of the crushing forces depends on the amount of contact between the relief face of the tool and the work material. The variation of contact during a crushing thrust of the tool was determined analytically by calculating the intersection of a tool edge with the workpiece (see figure 1.14). A MATLAB program calculated this intersection length. Figures 1.15 and 1.16 illustrate the variation of contact length *vs.* the vertical position of the tool for short and long tools for two wavelengths of vibration, 60 mil and 100 mil. Comparing with figures 1.11 and 1.12, we observe similarity in variation with crushing forces.

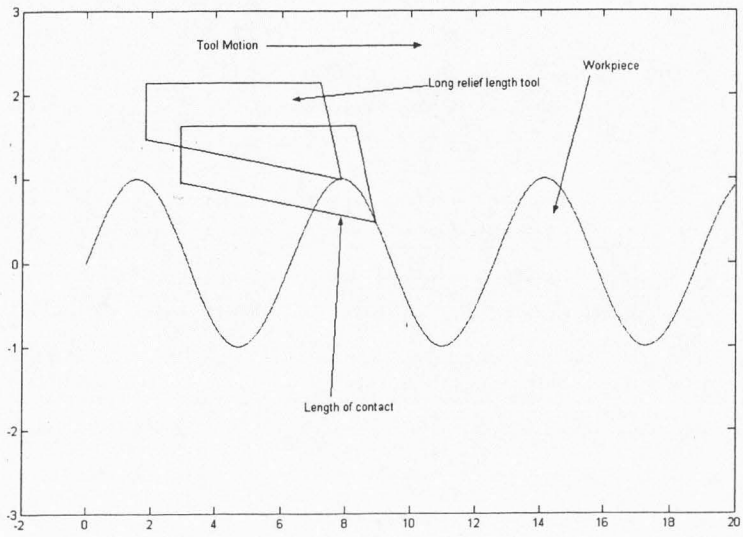

Figure 1.14. Contact Length calculation

Additionally we observe a direct dependence of maximum crushing force with wavelength for the long relief tool. This is the basis for modelling the crushing forces based on variation of contact length. Also observe saturation of contact length for the short relief tool and that this saturation length does not increase with decreasing wavelength, suggesting that a contact area model may work better in this case. Figure 1.17 is a plot of the crushing forces on the tool relief face and the contact length between the tool relief face and the workpiece *vs.* the vertical position of the tool for a long relief length tool (80 mil). The similarity between plots of contact length and crushing forces with position of tool suggested plotting of crushing forces vs. the contact length.

Figures 1.18, 1.19 and 1.20 are plots of the crushing force on the tool relief face vs. the contact length.

Referring to fig 1.18 for a long relief length tool (the multiple curves represent the fact that the tool has moved through more than one wavelength while cutting) , we see that the

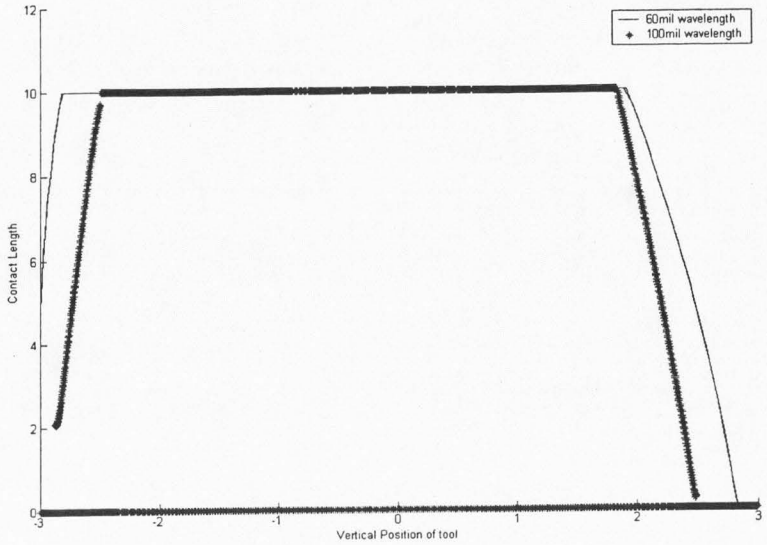

Figure 1.15. Contact Length vs. Vertical Position of short tool (10 mil)

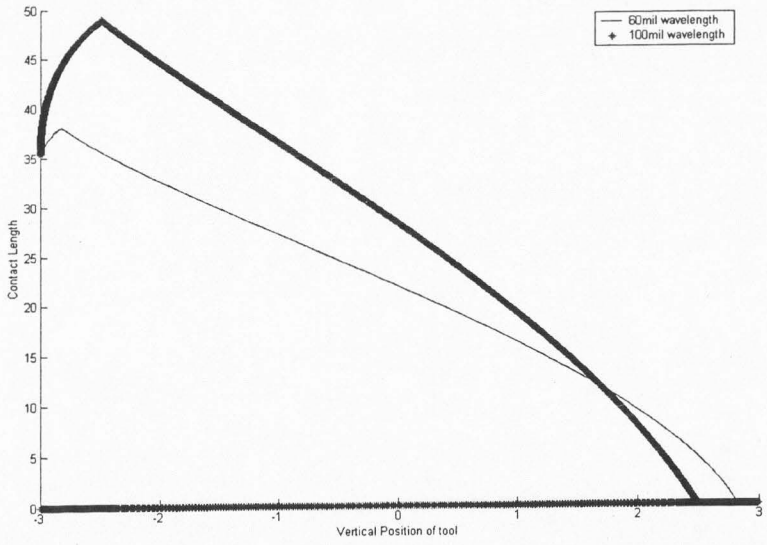

Figure 1.16. Contact Length vs. Vertical Position of long tool (80 mil)

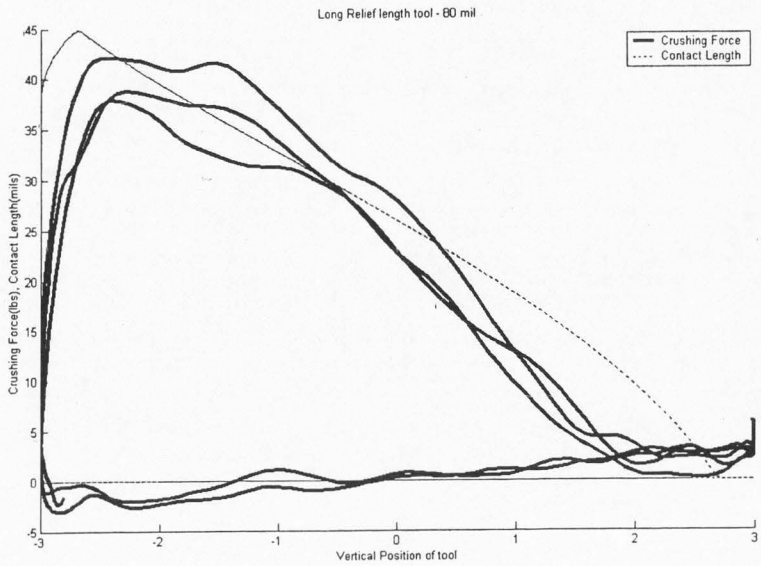

Figure 1.17. Crushing Forces and Contact Length vs. Vertical Position of tool

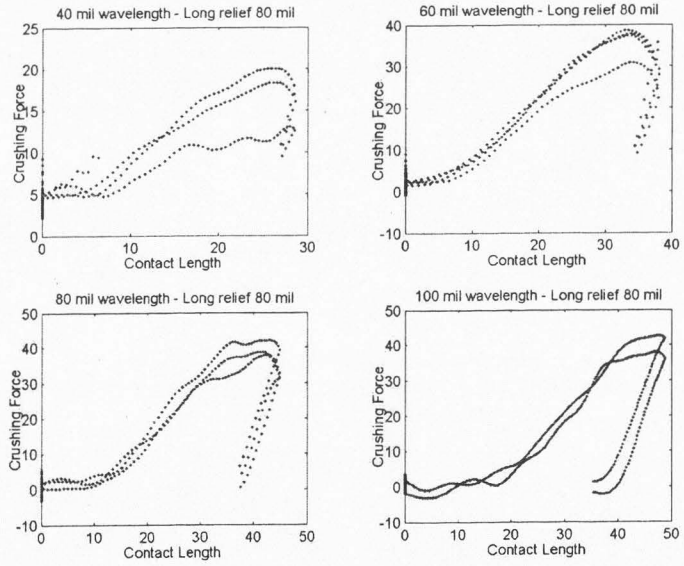

Figure 1.18. Crushing Forces vs. Contact Length - Long relief length tool (80 mil).

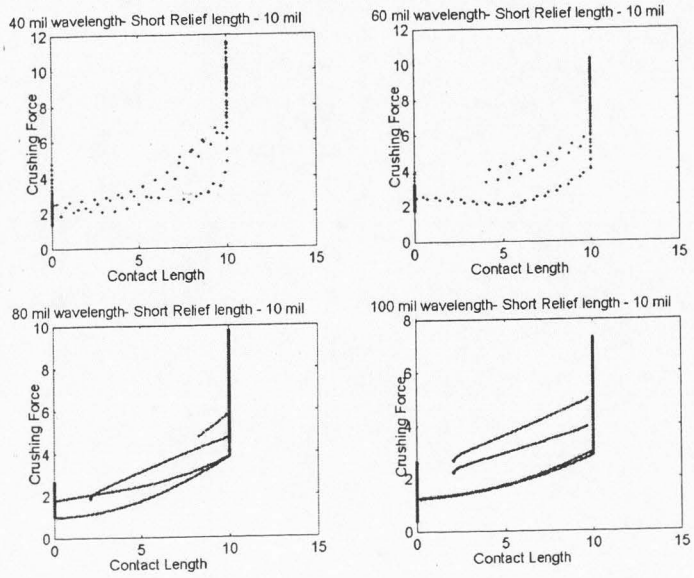

Figure 1.19. Crushing Forces vs. Contact Length - Short relief length tool (10 mil).

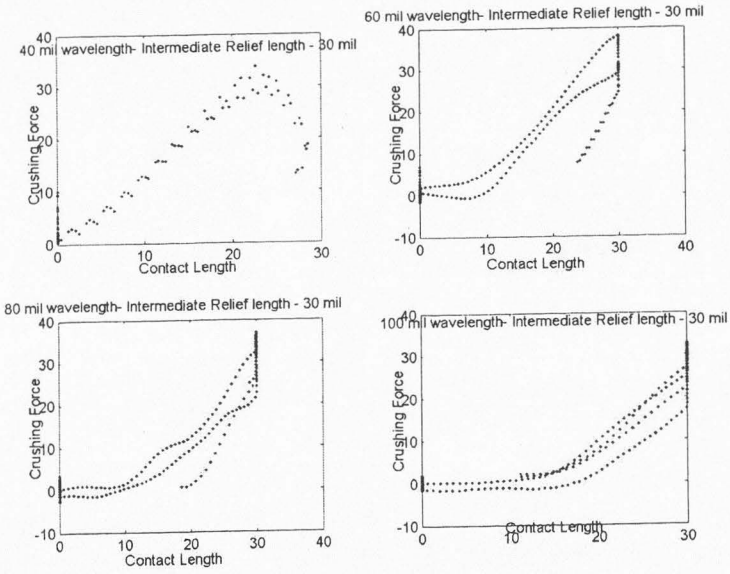

Figure 1.20. Crushing Forces vs. Contact Length - Intermediate relief length tool (30 mil).

relationship between the contact length and the crushing force is approximately linear in the mid portion of the curve between contact length values of 8 mil and 34 mil. For contact lengths higher than 34 mil curve does not show a linear relationship. The crushing forces decrease rapidly for a small decrease in the contact length. Refer again to figure 1.17. Recall that the loops are traversed counter-clockwise. Notice at the top of the loop, as the tool is about to move to its bottom-most position, the crushing forces start decreasing rapidly. However, the contact length still keeps increasing for a short while and then decreases more slowly than the decrease in crushing forces. This rapid decrease in crushing forces with a slow decrease in contact length explains the portion of figure 1.18 for contact lengths higher than approximately 34 mils. For a short relief length tool (see figure 1.19, the contact length between the relief face and the workpiece increases and then saturates at 10 mil (since the tool relief length is only 10 mil) at which point the tool is still moving down and the entire length of the relief face is in contact with the workpiece. We see from figure 1.19 that even though the contact length has saturated at 10 mil, the crushing forces continue to increase. This may be explained by the fact that while the contact length has saturated, area of material being crushed increases leading to higher crushing forces. Table 1.1 represents the linear fits of crushing force to contact length for different tool relief length and different wavelengths of vibration. y represents the crushing force and x, the explanatory variable is the contact length. The contact length and crushing force data used to obtain these fits was restricted to the middle portions of the plots of crushing forces vs. contact length where the relationship was approximately linear (between 10 and 34 mils for a long relief tool, between 0 and 10 mils for a short relief tool and between 10 and 25 mils for an intermediate relief tool).

1.4 MODELLING CRUSHING FORCES - CONCLUSIONS

1. We have modelled crushing behavior using AdvantEdge and investigated the behavior of crushing forces on the relief face of the tool (and on the work material at the same time) for varying tool relief lengths and varying wavelengths of vibration.

2. Brian Whitehead assumed an inverse relationship between the crushing forces and

Table 1.1. Linear fits of contact length and crushing forces.

Tool	Wavelength	Equation	Error (lbs)
Long relief length tool (80 mil)	40 mil	y = 1.1023*x + 0.39733	2.34
	60 mil	y = 1.13186*x - 1.5391	3.75
	80 mil	y = 1.1848*x - 9.6977	3.88
	100 mil	y = 1.30557*x -20.4926	3.74
Short relief length tool (10 mil)	40 mil	y = 0.5481*x + 1.5011	0.84
	60 mil	y = 0.2337*x + 1.3497	0.51
	80 mil	y = 0.20745*x + 1.484	0.12
	100 mil	y = 0.1672*x + 0.9573	0.33
Intermediate relief length tool (30 mil)	40 mil	y = 1.002*x + 3.6279	3.02
	60 mil	y = 1.4311*x - 6.4724	2.54
	80 mil	y = 0.9635*x -7.1277	2.47
	100 mil	y = 0.97697*x -7.877	2.62

the wavelength of vibration. We investigated this assumption and found that short relief length tools demonstrate this relationship. For long relief length tools, this relationship is inverted; maximum crushing forces demonstrate a direct dependence on the wavelength of vibration. The relationship is less clear for intermediate relief length tools. Note that given the wavelength of axial-torsional vibration typical of twist drills, the relief face is long compared to the wavelength and process damping models should take this into account.

3. We demonstrated that the length of contact between relief face of the tool and the workpiece shows similar variation as the crushing force and has similar relationships with the wavelength. Contact length was therefore used to model crushing forces.

4. We demonstrated an *approximately* linear relationship between the contact length and crushing forces for part of tool motion. This linear relationship does not hold during the initial descent of the tool into the workpiece and in the region just before the tool reaches its lowest position.

CHAPTER 2
DRILLING METAL STACKS

2.1 INTRODUCTION TO DRILLING METAL STACKS

Drilling is one of the most common operations used in the construction of an airplane. For example, a 747-400 needs about 3 million drilling operations in order to put in the fasteners used to hold the plane together. Boeing cuts composite materials and drills metal stacks to build airplanes. Any problems associated these operations can lead to increased costs. Composite materials allow lightweight design and structural performance because of lower weight, high strength and good fatigue performance. Metal stacks are clamped together; holes are drilled into them and the stacks are riveted together. Boeing is interested in modelling drilling operations in these situations and simulating associated problems. The original objective of this study was to model drilling of metal stacks and layered composites using AdvantEdge. However in order to compute the behavior of work material subjected to cutting forces AdvantEdge requires a material model (the relationship between the amount a material strains under the action of stresses). AdvantEdge does not currently support machining of composites because it does not have material models for composites.In this section we look at modelling drilling of metalstacks using AdvantEdge.

One of the most common problems encountered in the drilling of metal stacks is delamination (separation between layers). Other problems encountered during drilling are migration of chips into layer interfaces, crushing of layers, and burr formation, all of which reduce the strength of the material and hence its load carrying capacity [3]. This affects the structural integrity of aircraft, which are subjected to a combination of compressive, shear, fatigue and impact (e.g. bird-hits) loads during maneuvers.

Early studies on drilling of composites focused attention on delamination, matrix crack and fiber damage [4]. Other studies concentrated on preventive measures to reduce damage in the machined zone. Ho-Cheng and Dharan [1] identified thrust force as the principal

cause of delamination, described the two modes in which it acts, and derived a quantitative prediction of the onset of delamination as a function of the material properties and the uncut ply thickness. Their linear elastic fracture mechanics analysis was based on the presence of a circular crack in the material, which is propagated further due to the thrust forces of the drill.

Jain and Yang [8], [3] carried the work further by making the assumption that the initial crack was not circular but elliptical. Sadat [4] assumed planes of symmetry exist in the material and developed expressions for critical loads and feeds for delamination. All of these studies concentrated on the problem of delamination alone and did not consider other problems such as chip migration into interface, crushing of layers, and burr formation.

Two modes of delamination are *push-out-at-exit* and *peel-up-at-entrance*[1]. Let us analyze each.

The drill imposes a thrust force on the workpiece due to the feed, as it moves into the workpiece. As the drill approaches the end of the cut, the thickness of uncut material below the drill decreases, resulting in reduced stiffness and resistance to the thrust forces [1]. At a critical thickness, the thrust forces exceed the interlaminar bond strength, resulting in separation of the layers. This mechanism occurs close to the end of the hole and is therefore called the *push-out-at-exit* mode of delamination [Figure 2.1].

The second mechanism we examine is layer separation as the drill starts cutting into the workpiece. As the drill enters the workpiece, there is a tendency of the upper layers of material to move upwards along the flute. The material spirals up before it is machined completely [1] resulting in a peeling force which separates the upper layers from those layers which have not been cut as yet. Ho-Cheng and Dharan identify the peripheral force (due to rotation of drill) as the primary factor in creating this upward peeling away effect. Since

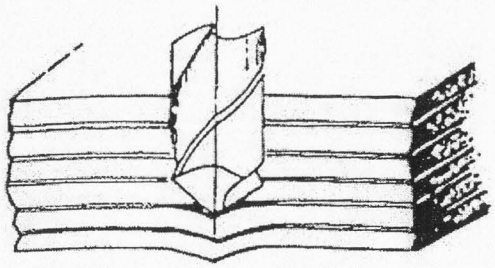

Figure 2.1. Push-Out-at-Exit Mode of Delamination [1].

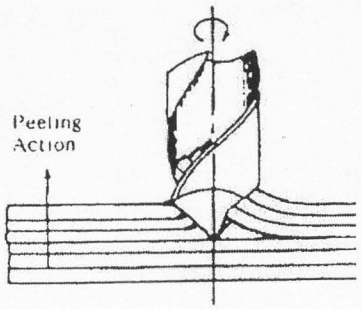

Figure 2.2. Peel-Up-at-Entrance Mode of Delamination [1].

it occurs at the start of the cut, it is called *peel-up-at-entrance* [Figure 2.2]. As the drill moves through the cut this mode of delamination decreases.

2.2 MODELLING DRILLING OPERATIONS

In this section we focus on modelling drilling. We note simplifying assumptions and consequent trade-offs. The modelling approach described is necessitated by features offered by AdvantEdge.

Drilling is a complex, three dimensional machining process due to the complicated shape and geometry of drilling tools and inserts. Drills require flutes to help remove cut material (see figure 2.3). The shape of these flutes results in a varying tool geometry along the cutting edge. Thus, in order to correctly model the drilling operation we must model the

motion of the drill as it cuts material in the workpiece and then account for changes in rake and relief angles along the cutting edge.

In modelling a physical process we balance the desire to capture all important characteristics against the need to make simplifications in order to make a complex problem more tractable. Simplifications we are making at this stage are related to current capabilities of AdvantEdge. AdvantEdge has the capability to simulate machining in both two and three dimensions. However, in three dimensions, it lacks the capability to simulate machining of workpieces which have layers. This necessitates transformation of the three dimensional drilling process to two dimensions. Additionally, AdvantEdge lacks the capability to create stacked workpieces with varying heights. This prevents modelling a tool that is subjected to a constant chip load (see figure 2.5) when cut at an angle.

The motion of a point on the drill cutting edge is the combination of two motions, rotation about the drill axis imparted to it through the spindle, and feed, so that the drill moves into the workpiece. Thus a point on the cutting edge moves in a helical path (figure 2.4).We transform the helical motion in 3D as shown in figure 2.4 to an equivalent motion in a plane. A point on the cutting edge at any instant of time during the cut will have two instantaneous velocities. One velocity will be the tangential velocity at the circumference due to the rotation. The other velocity will be velocity in the downward direction due to the feed (figure 2.4).

The drill is rotating at a constant rotational speed. Hence the tangential velocity ($V_{tangential}$ or V_x) of the point on the cutting edge under consideration must be constant (in magnitude) throughout the cut. The feed (V_{feed} or V_y) also remains constant. Note that the direction of the tangential velocity (V_x) vector changes as one moves along the motion path. Our main simplification in transforming to motion in a plane is to neglect the changing direction of the tangential velocity vector. In a plane the point under consid-

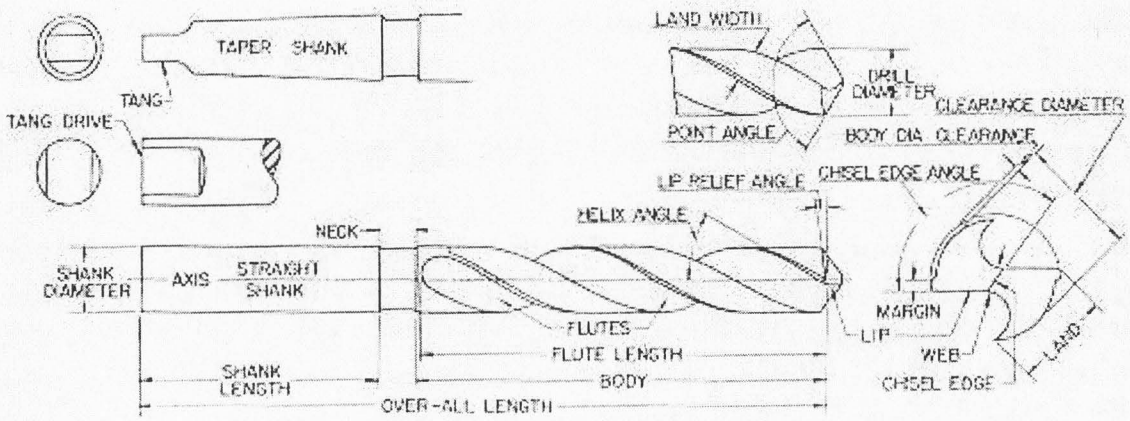

Figure 2.3. Twist drill geometry - two flutes (Sutherland, 2003)

eration would have the same two components of velocity whose directions are as shown in figure 2.4. One can think of this transformation from three dimensions to two dimensions as unwinding the helical motion such that the velocities along the cutting edge maintain the same magnitude.

V_x, the tangential velocity of the point along the cutting edge at a specified radius, given by

$$V_x = \omega * r \qquad (2.1)$$

where ω is the angular velocity of a point at a radius r from the central axis of the drill. (V_y) is the feed.

Figure 2.5 represents the transformed path of only one point along the cutting edge. The tool has the geometry of the actual tool that point. Figure 2.3 shows the flutes, the portion of the drill which is used for the evacuation of the chips. The shape of these flutes results in varying rake and relief angles along the cutting edge of the drill. To model cutting action at different points along the cutting edge, we select three points, one near the center of the drill along the cutting edge, one in the middle of the cutting edge and one at the

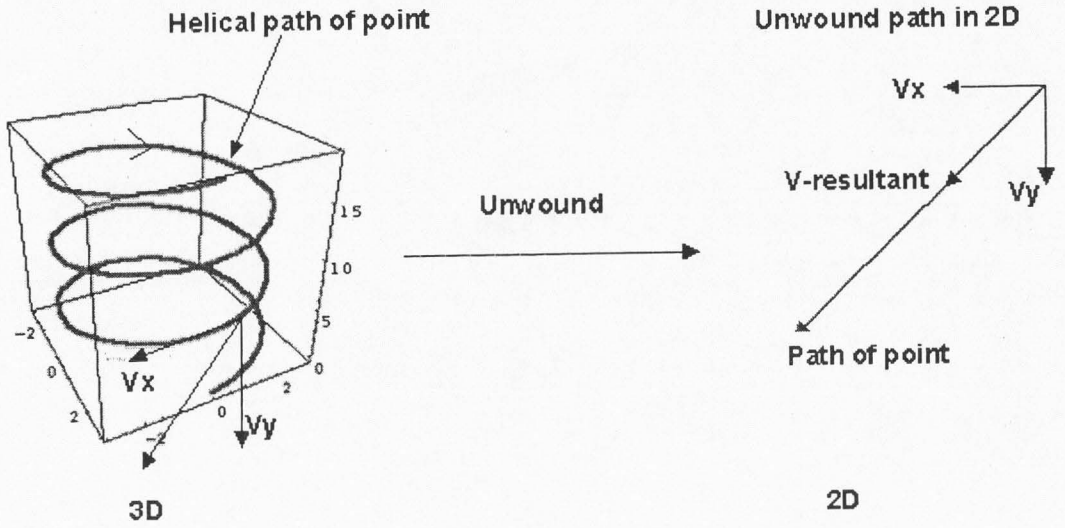

Figure 2.4. Transforming three dimensional motion to two dimensions.

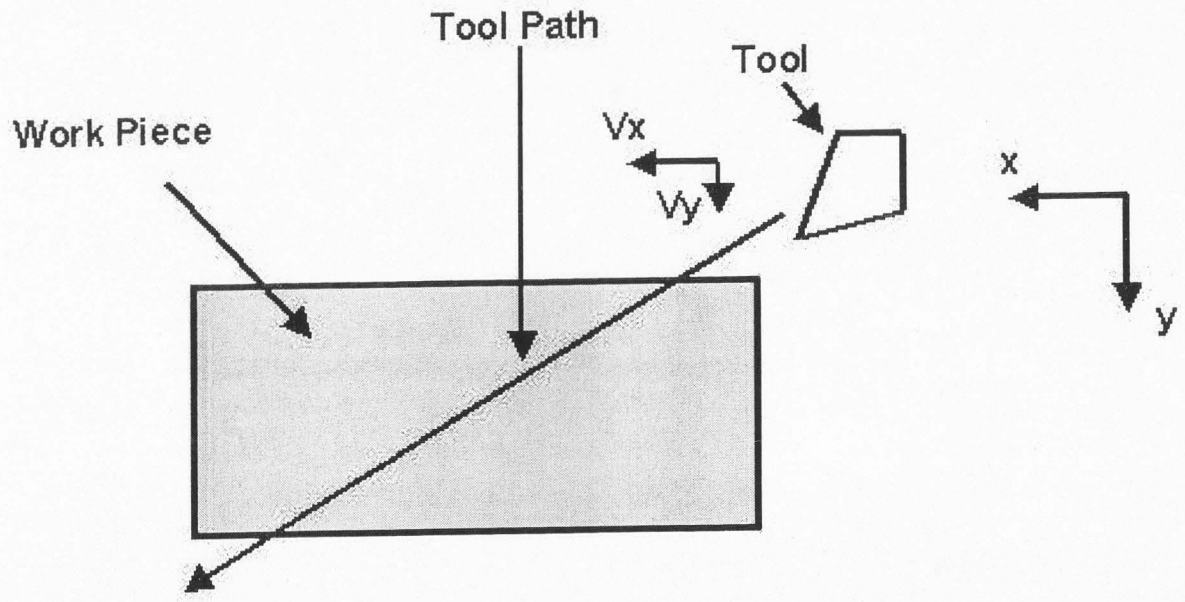

Figure 2.5. Tool Path and related velocities in two dimensions.

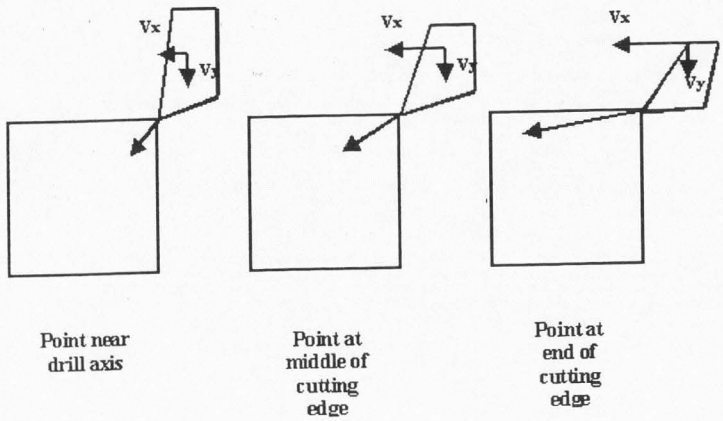

Figure 2.6. Variation of motion path for different points along cutting edge of drill.

outer end of the cutting edge. The paths of these points in our two dimensional model are represented as shown in the figure 2.6. Clearly the resultant path in two dimensions will be steepest for the point near the drill axis and the shallowest for the point at the end of the cutting edge.

The 2D model has the following limitations

1. Thrust force is the most important factor affecting delamination. It may depend on factors other than cutting speed, feed and tool geometry. The two dimensional model may not capture the effect of all factors.

2. In a drilling operation the drill is subjected to a constant chip load. In cutting at an angle the load on the tool increases. This is unrealistic. One way to eliminate this problem is to create a workpiece with a slant top so that the tool is always subjected to a constant chip load. However AdvantEdge lacks this capability. Varying chip load affects the forces on the work material.

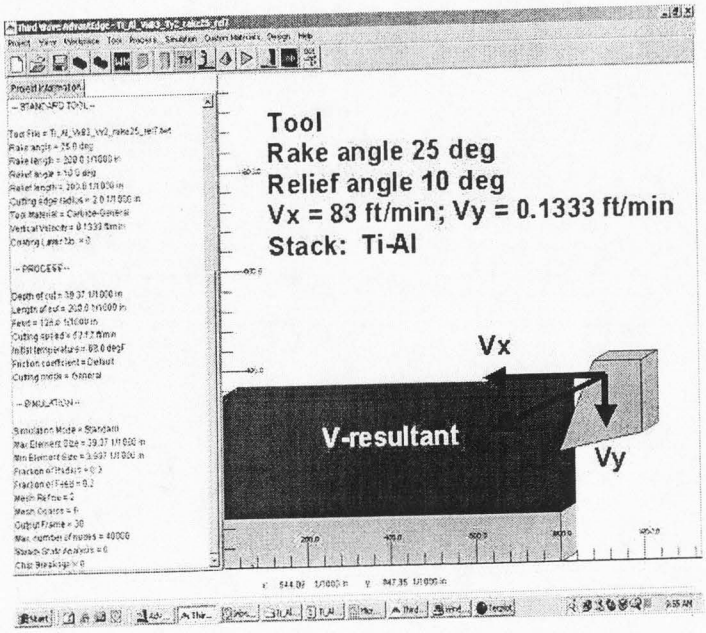

Figure 2.7. Typical Simulation set-up in AdvantEdge.

2.3 SIMULATING DRILLING OF METAL STACKS

2.3.1 Simulation Issues

Titanium-Aluminum (Ti-Al) stacks are commonly drilled in aircraft manufacture. AdvantEdge allows users to set up to 5 layers of metals. The boundaries between the layers are assumed to be in a state of perfect stick. Figure 2.7 represents a simulation with a layer of titanium and a bottom layer of aluminum. The tool is assumed to move from right to left. A drill has changing rake and relief angles along the cutting edge causing a change in thrust forces. We have run different two dimensional simulations for three points along the cutting edge of the same drill. Tool geometry at the selected points is calculated using a Boeing Internal Report [2] for a $\frac{1}{2}$" carbide drill. Given a rotational speed of drill and a feed, the tangential and feed velocities are computed at these points along the cutting edge. These velocities are inputs to the software. The effect of changing rake and relief on work material behavior is studied.

Recall from section 2.2 that we consider two modes responsible for the onset of delam-

Table 2.1. List of simulations.

Top($\frac{1}{4}$")	Bottom($\frac{1}{4}$")	Radius	(V_x)(ft/min)	(V_y)(ft/min)	Rake Angle	Relief Angle)
Al	Ti	0.2"	83	20	25	7
Ti	Al	0.2"	83	20	25	7
Al	Ti	0.025"	11	8	8	13
Al	Ti	0.125"	52	8	12	10
Al	Ti	0.2"	83	8	25	7
Ti	Al	0.025"	11	8	8	13
Ti	Al	0.125"	52	8	12	10
Ti	Al	0.2"	83	8	25	7

ination. The *push-out at exit* mode occurs when the thickness of the material below the drill is small. The *peel-up at entrance* mode occurs when the drill first enters the metal stack. We have therefore used small thickness for the layers in our simulations. Typical thicknesses of metal stacks are about a quarter of an inch. We use the same values in our simulations.

2.3.2 Simulation Parameters.

We chose three points along the cutting edge of a $\frac{1}{2}$" drill (at radii of 0.025", 0.125" and 0.2") and obtained approximate values of the rake and relief angles at these points using the Boeing Internal Report [2]. Table 2.1 shows tangential and feed velocities at these points as well as tool geometry. The workpiece used in this study consists of two layers of metal, titanium and aluminum. In each case the workpiece dimensions remained the same. We ran simulations with the layers in each order, Ti-Al or Al-Ti to observe differences in the cutting process.

The drill was assumed to rotate at a constant speed of 800 rpm. Typical feed velocities are in the range of a tenth of the tangential velocities (about 8 ft/min). However simulations run very slowly at this feed velocity. For this reason the feed velocity was increased for some of the simulations.

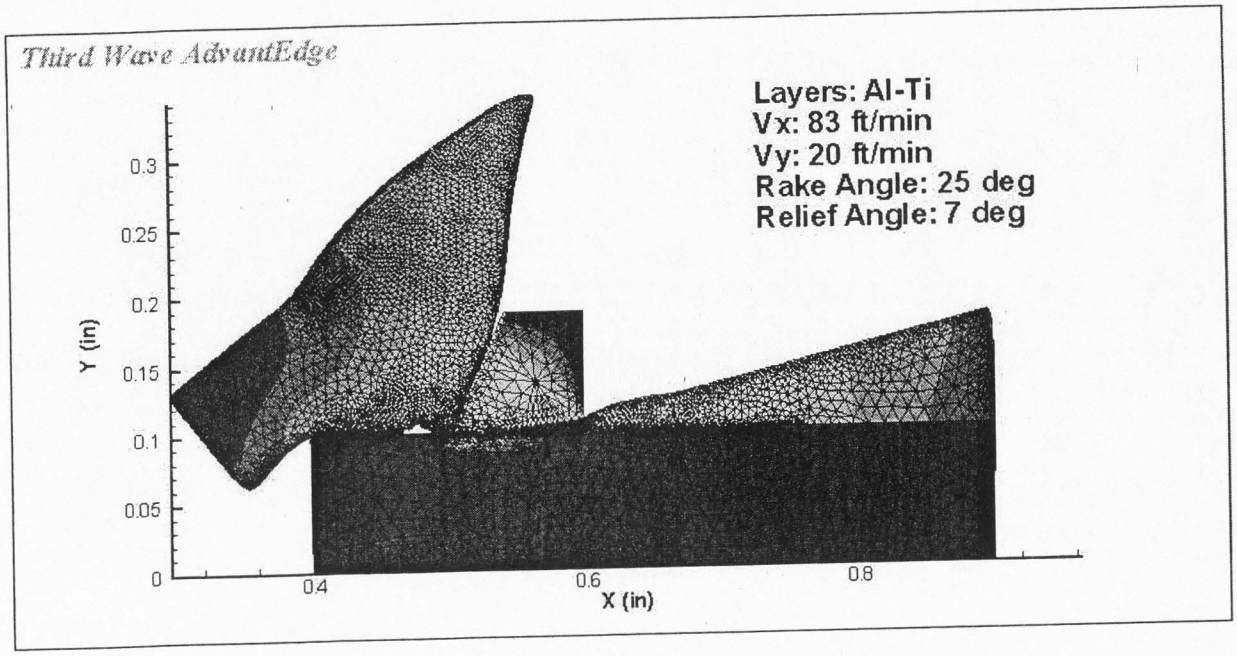

Figure 2.8. Al-Ti Stack - Rake Angle 25 Relief Angle 7

2.4 Results

We make the following observations based on our experience with simulations of machining of two layer stacks.

1. **Al-Ti Stack - Rake Angle 25 Relief Angle 7**

   Figure 2.8 is a frame from a simulation in which the top layer of the stack was Aluminum and the bottom layer was Titanium. Tool velocities are (V_x)= 83 ft/min and (V_x)= 20 ft/min. The top layer slides and folds over the bottom layer. The layers clearly have separated at the interface.

2. **Ti-Al stack - Rake Angle 25 Relief Angle 7** Figure 2.9 is a frame from a simulation in which the top layer of the stack was Titanium and the bottom layer was Aluminum. Tool velocities are the same as simulation 1 (Al-Ti Stack - Rake Angle 25 Relief Angle 7) . In this case the softer layer of aluminum gets crushed and slides under the titanium layer. A clear separation is seen in this simulation as well.

3. **Al-Ti stack - Rake Angle 12 Relief Angle 10** Figure 2.10 represents a machining

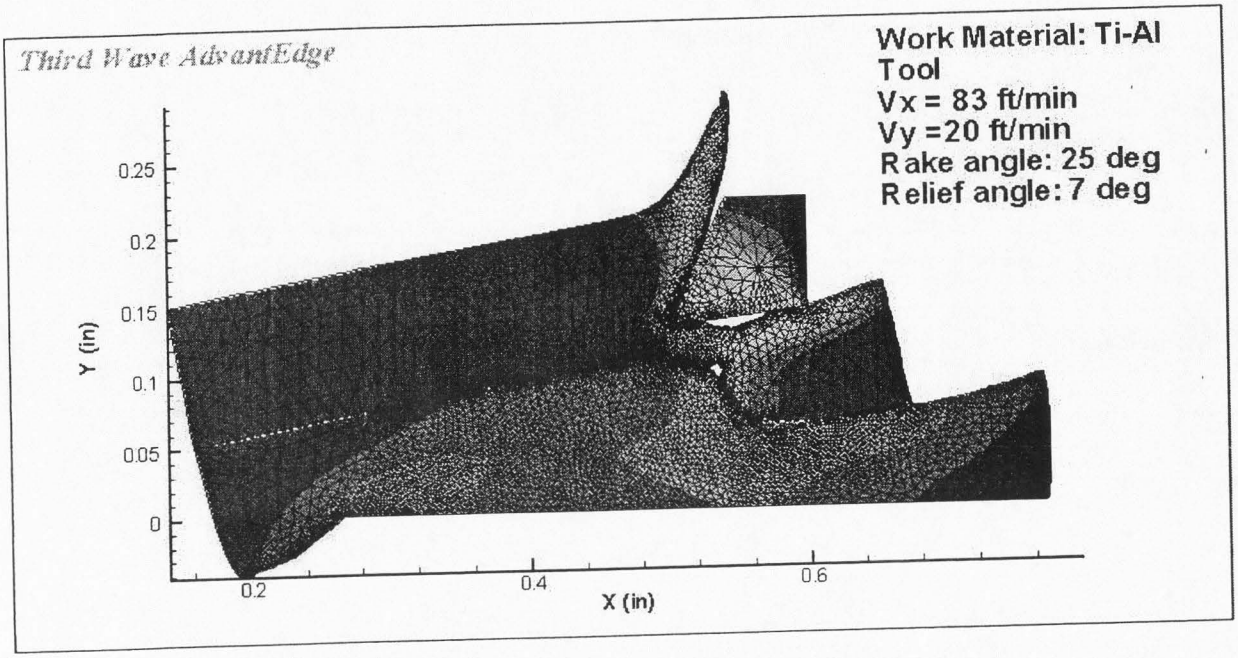

Figure 2.9. Ti-Al Stack - Rake Angle 25 Relief Angle 7

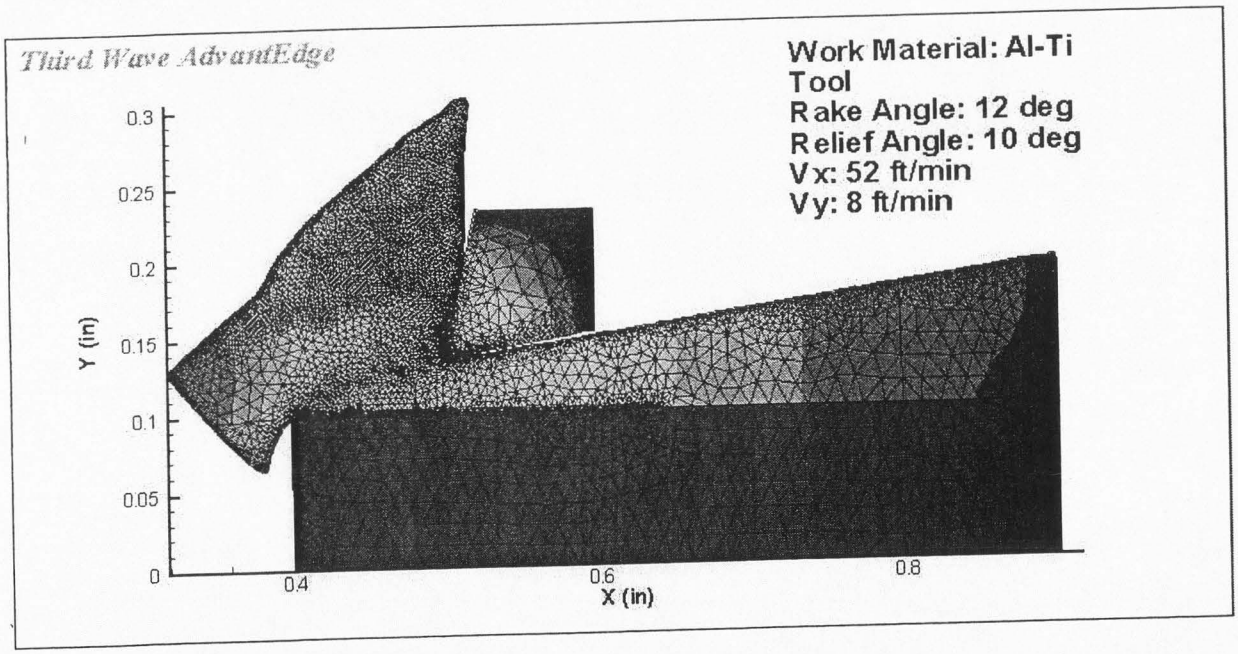

Figure 2.10. Al-Ti Stack - Rake Angle 12 Relief Angle 10

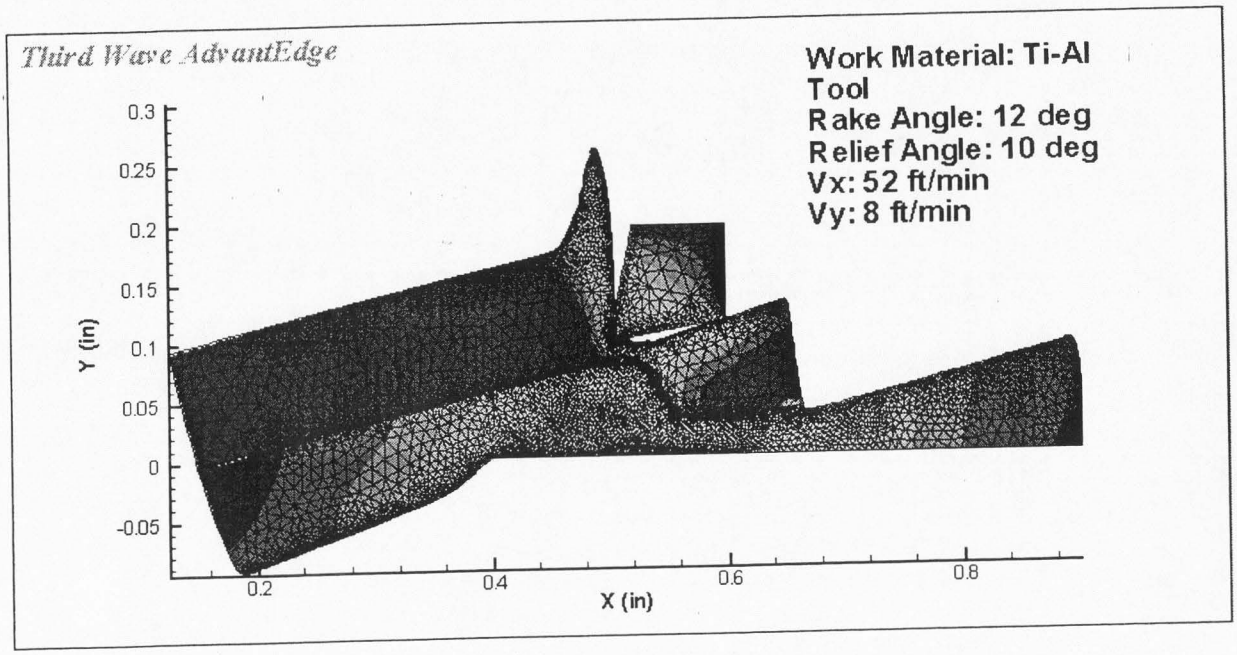

Figure 2.11. Ti-Al Stack - Rake Angle 12 Relief Angle 10

simulation on a Al-Ti stack. Tool velocities are (V_x)= 52 ft/min and (V_x)= 8 ft/min. At the specified tool velocities the aluminum layer is clearly sliding over the titanium layer. No separation is observed.

4. **Ti-Al stack - Rake Angle 12 Relief Angle 10** Figure 2.11 represents a machining simulation on a Al-Ti stack. Tool velocities are (V_x)= 52 ft/min and (V_x)= 8 ft/min. In this case, we observe squishing of the aluminum layer under the titanium layer and relative sliding between the layers.

5. **Al-Ti stack - Rake Angle 8 Relief Angle 13** Figure 2.12 represents a machining simulation on a Al-Ti stack at the point along the cutting edge closest to the drill axis. Tool velocities are (V_x)= 11 ft/min and (V_x)= 8 ft/min. The aluminum layer clearly slides under the tool and over the titanium layer. The varying chip load problem is evident here.

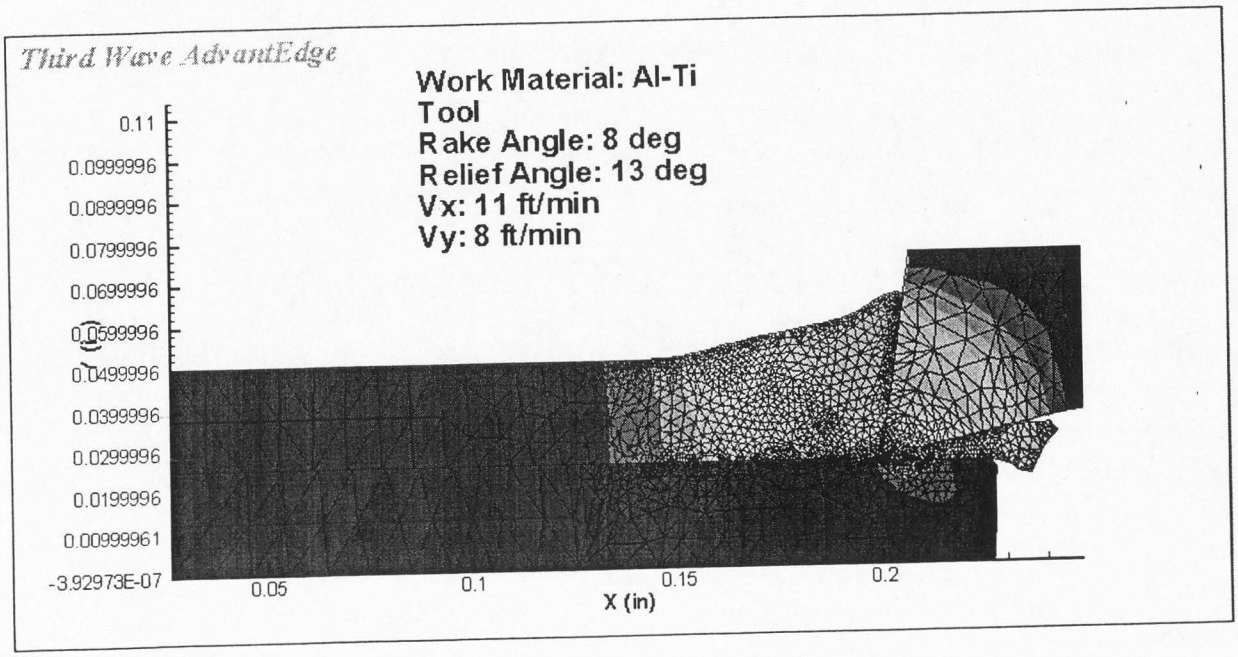

Figure 2.12. Al-Ti Stack - Rake Angle 8 Relief Angle 13

2.5 MODELLING DRILLING OF STACKS - CONCLUSIONS

1. Drilling may be transformed from a complex three dimensional process to a two dimensional one under simplifying assumptions mentioned in section 2.2.

2. From the results of section 2.4, we observe that metal layers initially in a state of perfect stick at the interface slide over each other or separate. At the interface high displacement values at nodes are probably resulting in a re-meshing, so that the perfect stick boundary condition does not hold any further and the layers may either slide relative to each other or separate.

3. Clearly moving along the cutting edge of the drill affects the thrust forces and consequently separation between layers. From the results of section 2.4, at the point on the cutting edge furthest away from the drill axis, the sharper rake angle and higher velocities resulted in a clear separation between layers in addition to relative sliding. Separation was not observed at the inner points along cutting edge, where tool ve-

locities were lower and rake angle was smaller. However some sliding between layers was observed. Thrust forces increase along the cutting edge and separation between layers may occur at outer ends of the cutting edge.

4. The simulations predict plausible behavior of the softer material (aluminum). When the top layer was aluminum, sliding and folding over the bottom titanium layer was observed. With titanium as the top layer, the softer bottom layer gets squished and slides under the top layer.

REFERENCES

[1] H. Ho-Cheng and C. Dharan, *Delamination during drilling in composite laminates*, J. of Eng for Industry, 112 (1990), pp. 236–239.

[2] Hodowany J. & A. Askari, *Cutting tool development: Modeling, design and performance analysis.* Boeing Internal Tech report-SSGTECH-98-022.

[3] S. Jain and D. Yang, *Delamination-free drilling of composite laminates*, J. of Eng for Industry, 116 (1993), pp. 475–481.

[4] A. Sadat, *Prediction of delamination load in drilling of graphite/epoxy composites*, American Society of Mechanical Engineers, Petroleum Division (Publication)PD, 75 (1996), pp. 21–27.

[5] E. Stone, A. Askari, and H. Tat, *Investigations of process damping forces in metal cutting.* Preprint.

[6] ThirdWave Systems Inc., *Thirdwave users manual v 4.3.*

[7] B. Whitehead, *The effect of process damping on stability and hole form in drilling*, master's thesis, Washington University, Saint Louis, Missouri, USA, 2001.

[8] D. Yang and S. Jain, *Effects of feed rate and chisel edge on delamination in composites drilling*, J. of Eng for Industry, 115 (1993), pp. 398–405.

APPENDICES

APPENDIX A

ADVANTEDGE NOTES

The following notes about running simulations with layers are useful in resolving run time problems.

1. Simulations running properly are listed in the job monitor. Absence of simulation name in the job monitor indicates failure of simulation, the reason for which can be obtained from the *.out file.

2. Outdated license files will lead to a checkout failed warning.

3. AdvantEdge may keep running in the background preventing usage of a simulation file. This may be prevented by ending the process in Task manager.

4. Batch simulations continue in the background even after process has been stopped. This may be prevented by stopping all simulations in the batch file that show up in the job monitor.

5. Folder or file names in AdvantEdge cannot have spaces. Additionally simulation file name must be the same as the folder name.

Run-time errors of the following types typically show up in simulations with layers.

1. Depending on simulation parameters, the specified number of nodes may be insufficient. Changes to the *.inp file help resolve this problem.

2. The adaptive meshing feature can fail either due to excessive mesh distortion or failure to identify surfaces. Increasing maximum number of nodes or decreasing the maximum element size value may be helpful in these situations. However by doing this we force excessive mesh refinement which may affect run times.